

# Analytical Camera Model Supplemented with Influence of Temperature Variations

Peter Podbreznik, Božidar Potočnik

**Abstract**—A camera in the building site is exposed to different weather conditions. Differences between images of the same scene captured with the same camera arise also due to temperature variations. The influence of temperature changes on camera parameters were modelled and integrated into existing analytical camera model. Modified camera model enables quantitatively assessing the influence of temperature variations.

**Keywords**—camera calibration, analytical model, intrinsic parameters, extrinsic parameters, temperature variations.

## I. INTRODUCTION

**A**N application for real-time activity tracking on the building site was developed as a pilot project. The differences between as-planned and as-built are recognized automatically from building site images [5]. Concept is based on comparison between real-time captured images and 4D model, made by 4D tool [6]. Building site is a dynamic environment, where also a temporary equipment (e.g. scaffolding stage, panellings) is the part of the building object during building process. Some parts of buildings are because of temporary equipment out of camera field of view. For this reason, the building site images should be captured from multiple cameras with fixed positions and orientations. Merging data from multiple cameras is possible, if the multiple camera system setup is calibrated. Calibration can be performed by various methods like: eight-point algorithm, LMedS, RANSAC, M-estimator, etc [2], [3], [9].

Temperature variations influence camera operation, because intrinsic and extrinsic camera parameters are changed. A change of extrinsic parameters appears as a change of geometrical properties of bearing structure with installed camera. Bearing structure actually expands due to temperature variations. On the other hand, a change of intrinsic camera parameters is reflected in a change of geometric properties of optical camera system.

The influence of temperature on camera was tested in project ESTEC [1]. A set of miniature cameras were exposed to extreme temperatures in thermal vacuum and a camera error was measured. The stability of camera system was very good and the measured error was round micron [1]. Calibrated low-cost CCD cameras were used in geodetic devices for distance measuring [4]. The measured distance error was 8 mm/°C [4]. Thermal low-cost CCD cameras were analyzed and small deviation of intrinsic camera parameters was detected in [7].

Changes of camera parameters due to the temperature variations are analysed and analytical camera model is modified in this article. A modification of perspective projection matrix  $\Delta\mathcal{M}$  is determined and an equation for particular camera

deviation is established. This error can be quantitatively calculated. Supplemented analytical camera model has been tested separately for intrinsic and extrinsic camera parameters.

This paper is organized as follows. In Section 2, an analytical camera model is reviewed, followed by a description of modified analytical camera model considering temperature variations influence in Section 3. Section 4 estimates temperature influence on camera with respect to a distance between camera and observed object. Results are presented and interpreted in Section 5. This paper concludes with some suggestions for future work.

## II. ANALYTICAL CAMERA MODEL

Transformation of spatial objects on image is defined by an analytical camera model. This transformation, which depends upon intrinsic and extrinsic camera parameters, are described as:

$$\mathbf{p} = \frac{1}{z}\mathcal{M}\mathbf{P}. \quad (1)$$

Parameter  $z$  is distance between normalized image plane and camera,  $\mathbf{p}$  is projection of spatial point  $\mathbf{P}$ , and  $\mathcal{M}$  is perspective projection matrix, defined as:

$$\mathcal{M} = \mathcal{K} \begin{pmatrix} \mathcal{R} & \mathbf{t} \end{pmatrix}, \quad (2)$$

where  $\mathcal{K}$  is calibration matrix,  $\mathcal{R}$  is rotation matrix, and  $\mathbf{t}$  is translation vector [2]. Intrinsic camera parameters are described by calibration matrix  $\mathcal{K}$ , while extrinsic camera parameters are defined by rotation matrix  $\mathcal{R}$  and translation vector  $\mathbf{t}$  [2], [9].

### A. Intrinsic parameters

Calibration matrix  $\mathcal{K}$  is in form of:

$$\mathcal{K} = \begin{pmatrix} f_\alpha & s & u_0 \\ 0 & f_\beta & v_0 \\ 0 & 0 & 1 \end{pmatrix},$$

where elements  $f_\alpha$ ,  $f_\beta$ ,  $u_0$ ,  $v_0$ , and  $s$  are intrinsic camera parameters. Parameters  $f_\alpha$  and  $f_\beta$  determine focus length, expressed in pixels. They are calculated as:

$$f_\alpha = kf \text{ and } f_\beta = lf, \quad (3)$$

where  $k$  and  $l$  are spatial resolution in  $x$  and  $y$  direction (unit pixel/m) and  $f$  is focus length. Parameters  $u_0$ ,  $v_0$ , and  $s$  define difference between coordinate systems of normalized plane and projective plane. Translation between coordinate systems is established by parameters  $u_0$  and  $v_0$ , depicted on image 1a. Skew parameter  $s$  define rotation angle  $\Theta$  of coordinate systems and is presented on image 1b [2].

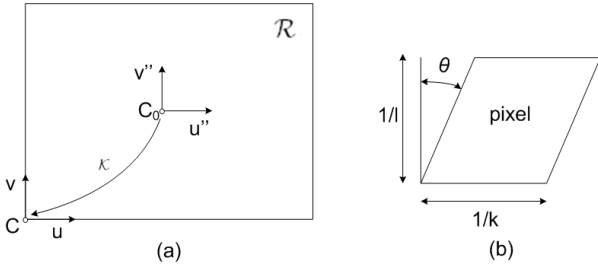


Fig. 1. Ascendance of intrinsic parameters during image transformation from normalized image plane into projective plane (a) and pixel form after rotation of coordinate systems of normalized image plane and projective plane (b).

### B. Extrinsic parameters

Perspective projection matrix  $\mathcal{M}$  is defined by equation (2). Extrinsic camera parameters (altogether six parameters) are obtained as the product of three elementary rotations and translation vector  $\mathbf{t}$ . Elementary rotation matrices are defined by three rotation angles  $\alpha$ ,  $\beta$  and  $\gamma$  around axes  $x$ ,  $y$  and  $z$ . The other three extrinsic parameters are components of translation vector  $\mathbf{t}$ , where  $\mathbf{t} = (t_x, t_y, t_z)$ .

### C. Perspective projection matrix $\mathcal{M}$

Equation (1) can be rewritten as  $z\mathbf{P} = \mathcal{M}\mathbf{P}$  or  $\mathbf{p} = \mathcal{M}\mathbf{P}$ , if projected spatial point  $\mathbf{P}$  has a form  $\mathbf{p} = (u, v, w)^T$ , where vectors component are defined as:  $u/w$  and  $v/w$ . The matrix  $\mathcal{M}$  consists of eleven independent camera parameters (i.e. five intrinsic and six extrinsic parameters). The full form of perspective projection matrix  $\mathcal{M}$  is:

$$\mathcal{M} = \begin{pmatrix} f_\alpha r_1^T + s r_2^T + u_0 r_3^T & f_\alpha t_x - s t_y + u_0 t_z \\ f_\beta r_2^T + v_0 r_3^T & f_\beta t_y + v_0 t_z \\ r_3^T & t_z \end{pmatrix}, \quad (4)$$

where  $r_1^T$ ,  $r_2^T$ , and  $r_3^T$  are rows of rotation matrix  $\mathcal{R}$ ;  $t_x$ ,  $t_y$ , and  $t_z$  are component of translation vector  $\mathbf{t}$ ; while parameters  $f_\alpha$ ,  $f_\beta$ ,  $u_0$ ,  $v_0$ , and  $s$  are intrinsic camera parameters.

## III. MODELLING INFLUENCE OF TEMPERATURE VARIATIONS

Camera on the building site is exposed to different weather conditions (e.g. rain, snow, temperature changes, wind). Normally, the camera is placed on a steel bearing structure. For such structure, we assume that it is homogeneous and the mass of camera do not influence on bearing structure. Variations of external temperature change the geometry of the bearing structure (i.e. provoke material expansion due temperature) and, consequently, extrinsic camera parameters are altered. The camera's optical system is exposed to external temperature as well, which influenced also intrinsic camera parameters. The influence of temperature variations on camera parameters are modelled in this sequel.

### A. Influence of temperature variations on intrinsic camera parameters

Five intrinsic camera parameters, i.e.  $f_\alpha$ ,  $f_\beta$ ,  $u_0$ ,  $v_0$ , and  $s$ , were defined in section II-A. We assume, the same temperature

inside a camera. Let us start with camera parameters  $f_\alpha$  and  $f_\beta$  defined by an equation (3). Temperature variations directly influence camera optical system and, consequently, alternation of camera focus length.

Linear material expansion is defined as:

$$\frac{dr}{r} = \psi dT, \quad (5)$$

where  $dr$  is length variation,  $r$  is material length,  $dT$  is temperature variation of material, and  $\psi$  is a linear temperature expansion coefficient of material [8]. In the same way, we modelled the variation of focus length as:

$$df = f\psi_f dT, \quad (6)$$

where  $f$  is focus length,  $\psi_f$  is temperature expansion coefficient of camera optical system, and  $dT$  is temperature variation. Very detail knowledge about camera optical system is required to exactly determine  $\psi_f$ . Usually, such camera optical system characteristics are not accessible.

Variation of focus length  $df$  directly influence parameters  $f_\alpha$  and  $f_\beta$  as:

$$f_{\alpha T} = k f_T,$$

where  $f_{\alpha T}$  is camera parameter after temperature was changed. The new focus length  $f_T$  is thus:

$$f_T = f_{T_0} + \Delta f_{T_r},$$

where  $f_T$  is focus length after temperature variation,  $f_{T_0}$  is camera focus length at normal temperature, and  $\Delta f_{T_r}$  is focus length variation due to temperature variation. Parameter  $f_{\alpha T}$  could be rewritten in expanded form as:

$$f_{\alpha T} = k f (1 + \psi_f dT). \quad (7)$$

Camera parameter  $f_\beta$  is defined on the same way like:

$$f_{\beta T} = l f_T \quad \text{and} \quad f_{\beta T} = l f (1 + \psi_f dT)$$

where  $f_{\beta T}$  is camera parameter after temperature variation and  $l$  denotes spatial resolution ( $1/l$  determines pixel's height). Factors  $k$  or  $l$  and focus length  $f$  are inversely proportional. Thus, parameters  $f_\alpha$  and  $f_\beta$  from equation (3) are constant—if camera settings stay unchanged—and independent of focus length variations, and, consequently of temperature variations.

Intrinsic camera parameters are also parameters  $u_0$ ,  $v_0$ , and  $s$ . Parameters  $u_0$  and  $v_0$  describe translation between coordinate systems of normalized and projection plane. If temperature varies uniformly over a camera, the geometry of optical system changes proportional as well and has no influence on camera's functionality. The same consideration is true for a skew parameter  $s$ .

### B. Influence of temperature variations on extrinsic camera parameters

Six extrinsic camera parameters have been defined in Section II-B, i.e. the three angles defining rotation matrix  $\mathcal{R}$  and the three coordinates of translation vector  $\mathbf{t}$ . Extrinsic camera parameters are defined by camera position and orientation. A variation of bearing structure directly influences a camera position and, consequently, results in modification of extrinsic

camera parameters. Each bearing structure must be analysed individually. Simplified model, presented by construction vector  $\mathbf{v}_s$  (Fig. 2), could be used for homogenous bearing structure.

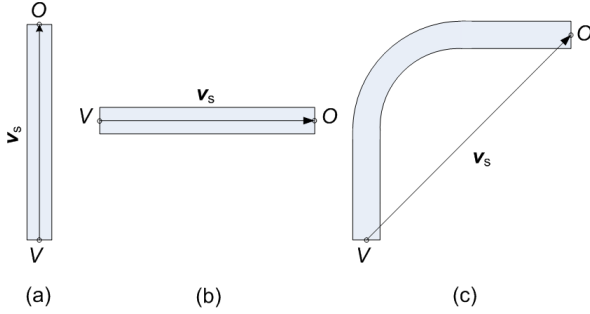


Fig. 2. Construction vector  $\mathbf{v}_s$  of bearing structure extends from starting point  $V$  and camera mounting point  $O$ . Different bearing structures like: column (a), beam (b) and composition of column and beam (c).

Translation vector  $\mathbf{t}$  at temperature  $T$ , denoted as  $\mathbf{t}_T$ , is written as:

$$\mathbf{t}_T = \mathbf{t}_{T_0} + \Delta\mathbf{t}_{T_r} \quad (8)$$

where  $\mathbf{t}_{T_0}$  is translation vector at normal temperature  $T_0$  and  $\Delta\mathbf{t}_{T_r}$  is a variation of translation vector, expressed as:

$$\Delta\mathbf{t}_{T_r} = \mathbf{v}_s \psi dT, \quad (9)$$

where  $\mathbf{v}_s$  is the construction vector at normal temperature  $T_0$ ,  $\psi$  is a linear temperature expansion coefficient, and  $dT$  is a temperature variation. Linear temperature expansion coefficients can be read from tables, e.g. [8]. Rotation of camera is not possible, since homogenous bearing structure expands in all directions equally. Variation of bearing structure depends, thus, only on construction vector  $\mathbf{v}_s$  (see equation (9)).

### C. Modification of analytical camera model

Findings from previous two subsections are included in analytical camera model. The perspective projection matrix is supplemented by a term for measuring variations of extrinsic camera parameters. Analytical camera model from equation (2) assures perspective projection without deviation (i.e. error) at normal temperature. Deviations arise with a change of geometrical properties of bearing structure.

Perspective projection matrix  $\mathcal{M}$  supplemented with an influence of temperature variations, results in a new perspective projection matrix  $\mathcal{M}_T$ , defined as:

$$\mathcal{M}_T = \mathcal{K} \left( \mathcal{R} + \Delta\mathcal{R}_{T_r} \quad \mathbf{t} + \Delta\mathbf{t}_{T_r}, \right), \quad (10)$$

where  $\mathcal{R}$  is rotation matrix,  $\Delta\mathcal{R}_{T_r}$  is variation of rotation matrix,  $\mathbf{t}$  is translation vector, and  $\Delta\mathbf{t}_{T_r}$  is variation of translation vector. Equation (10) can be rearranged as:

$$\mathcal{K} \left( \mathcal{R} + \Delta\mathcal{R}_{T_r} \quad \mathbf{t} + \Delta\mathbf{t}_{T_r}, \right) = \mathcal{K} \left( \mathcal{R} \quad \mathbf{t}, \right) + \mathcal{K} \left( \Delta\mathcal{R}_{T_r} \quad \Delta\mathbf{t}_{T_r}, \right).$$

The matrix  $\mathcal{M}_T$  written in a short form is:

$$\mathcal{M}_T = \mathcal{M} + \Delta\mathcal{M}, \quad (11)$$

where  $\mathcal{M}_T$  is the perspective projection matrix at temperature  $T$ ,  $\mathcal{M}$  is the normal perspective projection matrix from equation (4), and matrix  $\Delta\mathcal{M}$  is a variation of perspective projection matrix due to temperature change  $dT$ .

Translation vector  $\mathbf{t}$  only is changed due to temperature variations (see Sections III-A and III-B). Therefore, the variation of perspective projection matrix  $\Delta\mathcal{M}$  converts into:

$$\Delta\mathcal{M} = \mathcal{K} \left( \mathbf{0}_{3,3} \quad \Delta\mathbf{t}_{T_r}, \right), \quad (12)$$

where  $\mathbf{0}_{3,3}$  is  $3 \times 3$  zero matrix and  $\Delta\mathbf{t}_{T_r}$  is a variation of translation vector  $\mathbf{t}$ .

Finally, the perspective projection matrix  $\mathcal{M}_T$  of analytical camera model supplemented with an influence of temperature variations, written in expanded form, is:

$$\mathcal{M}_T = \begin{pmatrix} f_\alpha \mathbf{r}_1^T + s \mathbf{r}_2^T + u_0 \mathbf{r}_3^T & f_\alpha t_{T_x} - s t_{T_y} + u_0 t_{T_z} \\ f_\beta \mathbf{r}_2^T + v_0 \mathbf{r}_3^T & f_\beta t_{T_y} + v_0 t_{T_z} \\ \mathbf{r}_3^T & t_{T_z} \end{pmatrix}, \quad (13)$$

where  $f_\alpha$ ,  $f_\beta$ ,  $s$ ,  $u_0$ , and  $v_0$  are intrinsic camera parameters;  $\mathbf{r}_1^T$ ,  $\mathbf{r}_2^T$ , and  $\mathbf{r}_3^T$  are the rows of rotation matrix  $\mathcal{R}$ ; and  $t_{T_x}$ ,  $t_{T_y}$ , and  $t_{T_z}$  are coordinates of translation vector  $\mathbf{t}_T$ , calculated from equation (8).

This model will be experimentally verified in Section V.

## IV. CAMERA MODEL AND ESTIMATION OF ERROR MAGNITUDE

Extrinsic camera parameters are changed due to temperature variations if camera is located on building site. We set an expected camera working range for easier error magnitude prediction of camera exposed to temperature variations on building site. The following assumptions are made:

- temperature is between  $0 - 40^\circ\text{C}$ ,
- bearing structure is homogenous and steely,
- a length of steel bearing structure is under three meters, and
- distance between observed objects and camera is more than ten meters.

Temperature variations provoke a translation of bearing structure for vector  $\Delta\mathbf{t}_{T_r}$  in direction of the construction vector  $\mathbf{v}_s$ . Coordinates of translation vector  $\Delta\mathbf{t}_{T_r}$  (equation (9)) in projection plane must be calculated. The third coordinate of this vector should be set to zero, because it has no influence on error (see Section III-A). To determine a projection of translation vector  $\Delta\mathbf{t}_{T_r}$ , an angle  $\phi$  between normal vector of projection plane, i.e. vector  $\mathbf{n}_p$ , and vector  $\Delta\mathbf{t}_{T_r}$ , must be calculated from the following equation:

$$\cos \phi = \frac{\mathbf{n}_p \Delta\mathbf{t}_{T_r}}{\|\mathbf{n}_p\| \|\Delta\mathbf{t}_{T_r}\|}.$$

Angle  $\phi$  is the angle between  $\mathbf{n}_p$  and  $\Delta\mathbf{t}_{T_r}$ ,  $\|\cdot\|$  denotes vector length. A projection of vector  $\Delta\mathbf{t}_{T_r}$ , denoted as  $\Delta\mathbf{t}_{T_r}^p$ , is then calculated according to a prescription (see also Fig. 3):

$$\Delta\mathbf{t}_{T_r}^p = \sin \phi \Delta\mathbf{t}_{T_r} \text{diag}(1, 1, 0), \quad (14)$$

where  $\text{diag}(1, 1, 0)$  denotes a  $3 \times 3$  diagonal matrix.

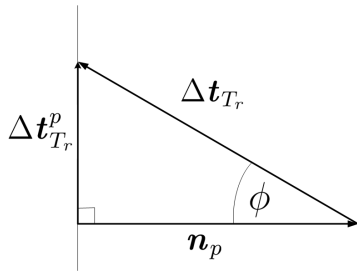


Fig. 3. Projection of translation vector  $\Delta t_{T_r}$ , denoted as  $\Delta t_{T_r}^p$ .

A result of equation (14) can not be directly applied on images. For this reason, the projection  $\Delta t_{T_r}^p$  must be expressed in pixel units. The following procedure is suggested:

- estimate parameters  $k$  and  $l$  (i.e. count out the number of pixels per distance unit),
- determine a focus length  $f$  (i.e. estimate a distance between camera and observed object), and
- calculate intrinsic camera parameters  $f_\alpha$  and  $f_\beta$  by using equation (3).

Parameters  $f_\alpha$ ,  $f_\beta$ , and distance to the observed object, denoted as  $r$ , suffice to determine an object size in pixels for any object on image. On the same way, it is possible to determine an error magnitude (expressed in pixels) for all observed object pixels. Error magnitude means a deviation of measured pixel position from its correct position. It should be stressed that this error is due to vector  $\Delta t_{T_r}$ . Error magnitude for axis  $x$  is calculated as:

$$N_x = \Delta t_{T_{rx}}^p \frac{f_\alpha}{r} \quad (15)$$

and for axis  $y$  as

$$N_y = \Delta t_{T_{ry}}^p \frac{f_\beta}{r}, \quad (16)$$

where  $\Delta t_{T_{rx}}^p$  and  $\Delta t_{T_{ry}}^p$  are coordinates of projection vector  $\Delta t_{T_r}^p$  (equation (14)). Values  $N_x$  and  $N_y$  denote error magnitude in pixels on image plane, as is depicted in Fig. 4. Mark  $P_0$  denotes correct pixel position (e.g. at normal temperature), while  $P_T$  denotes the same pixel translated due to temperature variations (i.e. position of pixel at temperature  $T$ ).

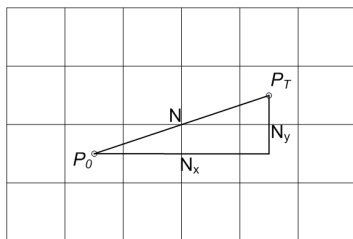


Fig. 4. Error magnitude, denoted as  $N_x$  and  $N_y$ , presented on image plane.

The total error magnitude is, thus, defined as:

$$N = \sqrt{N_x^2 + N_y^2}. \quad (17)$$

Values  $N_x$  or  $N_y$  and distance to the observed object from a camera are inversely proportional (equations (15) and (16)). Therefore, if distance to the observed object is greater than ten meters and if camera works in its expected working range, then error magnitude is less than pixel.

## V. RESULTS

Modified analytical camera model was tested in four experiments. Expected error magnitude calculated from analytical model was compared to measurements performed directly on images. Environment temperature variations were simulated in these experiments. First, let us define a term "normal point". Normal point is the observed point on the image at normal temperature  $T_0 = 20^\circ\text{C}$ . Points, calculated with the analytical model without temperature variations, theoretically have the same positions as the normal points (the only error is due to an accuracy of used camera model). The deviation between observed and predicted normal points, expressed in pixels, are presented in table I. Predicted normal points positions were calculated from equation (17) and compared with normal point positions measured directly on image. Performed experiments are described more in detail in this sequel.

### A. The first experiment

This experiment was performed by using 3 meters long steel bearing structure and camera Canon PowerShot A85. Structure was layed down on the floor and one of its ends was fixed. The camera was mounted on right side of bearing structure and placed one meter from the observed point  $P$ , as depicted in Fig. 5. It was planned to take image of observed points  $P$  in temperature range 0 to  $40^\circ\text{C}$ , every  $5^\circ\text{C}$ .

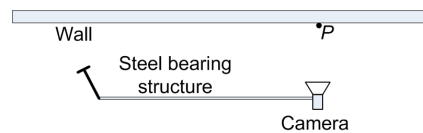


Fig. 5. Ground plan view of bearing structure fixed on the left and with the camera on the right side. Observed point  $P$  was fixed on the wall.

This experiment was performed in an experimental room. Several problems merged during experiment:

- expected temperature range couldn't be reached, because a thermal accumulation in the walls and floor was too high,
- thermal losses prevent reaching temperature of  $40^\circ\text{C}$  in experimental room.

Because of above mentioned problems, the experiment was started at  $5^\circ\text{C}$  and was interrupted at  $25^\circ\text{C}$ . Robustness of bearing structure and very small change of translation vector  $\Delta t$  are reasons, that observed point position  $P$  at temperature  $T$  did not deviate noticeable from normal point. A thermal chamber is necessary to make such experiment complete.

**B. The second experiment**

An alternation of extrinsic camera parameters directly influence camera position (see equation (8)). Camera position change can be exactly determined for known temperature variation, if the bearing structure is homogenous. This experiment focus was, therefore, on the intrinsic camera parameters. A special experimental environment, isolated from surroundings, was designed. The lateral view of this environment with mounted camera and observed point  $P$  is depicted in Fig. 6. Experimental environment is portable. This enables us to make

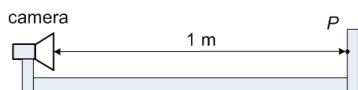


Fig. 6. Lateral view of experimental environment with camera and observed point  $P$ .

experiment on open air at  $0^{\circ}\text{C}$  and also in sauna at  $50^{\circ}\text{C}$ .

Both acquired images, see Figs 7c and 7d, were analyzed and the number of pixels between black lines (see detail view in Figs 7a and 7b) were counted out. It pointed out that the number of pixels were the same in both images. We can conclude that the temperature variation in the temperature range  $0$  to  $50^{\circ}\text{C}$  did not noticeable influence intrinsic camera parameters. Several cameras were used in this experiment (e.g. Cannon PowerShot A85, Cannon Ixus 300, and Olympus MJU 750).

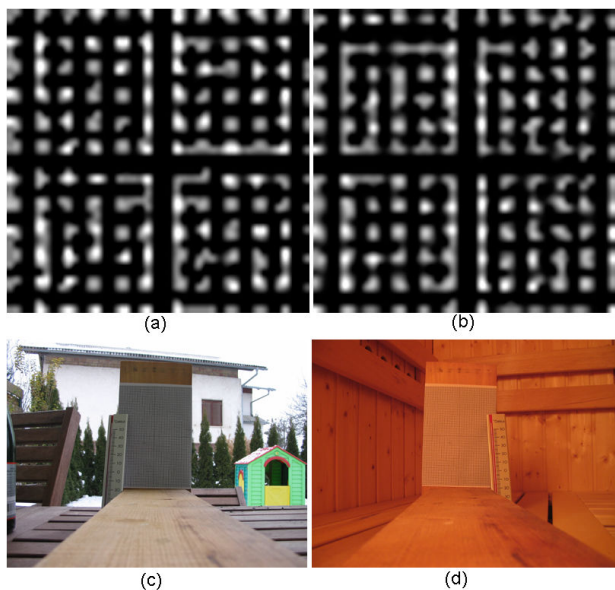


Fig. 7. Enlarged image of graph paper of size  $20 \times 20$  mm, acquired at temperature a)  $0^{\circ}\text{C}$  and b)  $50^{\circ}\text{C}$ ; c) and d) are corresponding original images.

**C. The third experiment**

The third experiment was performed as follows. One meter long, steel bearing structure was fixed in point  $V$  and the

camera was placed on this structure at point  $O$  (see Fig. 8). Camera's field of view is perpendicular to the construction vector  $v_s$ . Observed point  $P$  has fixed location. Point  $V$  and direction from points  $V$  to  $O$  is also fixed. The position of point  $O$  changes in direction of the construction vector  $v_s$  with respect to temperature variations, structure length, and temperature expansion coefficient.

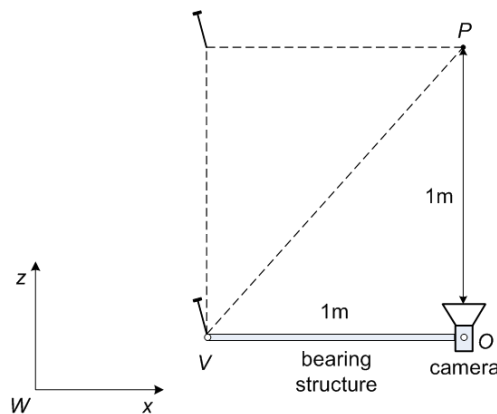


Fig. 8. The scheme of portable experimental environment, where camera is placed on bearing structure at point  $O$ ,  $P$  is observed point, and bearing structure is fixed at point  $V$ .

This experimental environment was portable as well. Such design, see Fig. 8, enables us to set this device on different locations and by different temperature conditions. However, in practice it was impossible to set up position of points  $V$  and  $P$  completely accurately. This error was in the same range as expected error magnitude due to temperature variations. Polyester fibers were used for a determination of point locations.

Experiment pointed out that is impossible to completely accurately re-set experimental environment (especially location of points  $P$  and  $V$ ), because measuring devices are influenced by temperature variations in the same manner as camera bearing structure. Physical facts lead us to the same conclusion as in the first experiment, i.e. fixed experimental environment, which can be put into thermal chamber.

**D. The fourth experiment**

We separately analysed intrinsic and extrinsic camera parameters in the fourth experiment. At the end, intermediate results were merged into final findings. The intrinsic camera parameters were measured independently of extrinsic parameters and no temperature influence was noticed (see the second experiment). Extrinsic camera parameters are influenced only by variation of the construction vector  $v_s$ . As shown in Section III-B, we are able to exactly model this behaviour of bearing structure. With this experiments we will verify statements about intrinsic and extrinsic camera parameters.

Measurements were performed by counting out a deviation (in pixels) from correct observed point position and compared with the expected error magnitude calculated from equations (15) and (16). The camera position (translation vector  $\Delta t_{T_r}$ )

was changed manually in direction  $x$  and  $y$ . To obtain more accurate results, the translation vector  $\Delta t_{T_r}$  was changed for larger distances as expected on the building site due to temperature variations. Measured and calculated deviations (in pixels) are presented in table I for different distances  $r$ , i.e. distance between camera and observed objects. The camera with intrinsic parameters  $f_\alpha = f_\beta = 1643$  was used in this experiment. When the distance  $r$  is smaller than half a meter, a bigger discrepancy between measured and calculated values was noticed. The reason for this is that camera optical system is not designed for acquiring image at very small focus length. The measured and calculated values match for distances  $r$  longer than meter.

TABLE I

DEVIATION (IN PIXEL) FROM CORRECT OBSERVED POINT POSITION. COLUMNS  $N_{dev}^c$  PRESENT CALCULATED RESULTS BY USING OUR CAMERA MODEL AND COLUMNS  $N_{dev}^m$  PRESENT MEASURED RESULTS. MARK  $dev$  DENOTES A CAMERA TRANSLATION FOR 1, 10 AND 50 MM IN BOTH DIRECTIONS ( $x$  AND  $y$ ), WHILE  $r$  IS A DISTANCE FROM CAMERA.

$r$ [m]	$N_1^c$	$N_1^m$	$N_{10}^c$	$N_{10}^m$	$N_{50}^c$	$N_{50}^m$
0,5	3,34	2	33,4	32	167	158
1	1,67	2	16,7	17	83,5	83
2	0,83	1	8,35	8	41,75	41
5	0,33	1	3,34	4	16,70	17
50	0,03	0	0,33	0	1,67	2

Finally, let us summarize findings based on our experiments. Influence of temperature variations on extrinsic camera parameters was modelled in Section III-A and experimentally confirmed in the second experiment. Our modified analytical camera model actually includes the deviation of extrinsic camera parameters as a modification of translation vector  $t$ . We also derive a formula (equation (17)) for calculating error magnitude with respect to the variation of translation vector  $\Delta t_{T_r}$ . The measured and calculated deviations are presented in table I. For observed objects at distance more than meter from camera both results match. Based on all experiments we state that our modified analytical camera model, defined by equation (13), is confirmed.

## VI. CONCLUSION

Analytical camera model has been modified with an influence of temperature variations on camera working in this paper. It was confirmed by experiments that temperature variations in expected camera working range on building site have no influence on intrinsic camera parameters. Camera is usually placed on steel bearing structure on the building site. With temperature changing, this structure changes its geometrical properties and, consequently, a translation vector  $t$  is changed. Modified analytical camera model comprehends also a change of extrinsic camera parameters due to temperature variations. Proposed camera model was confirmed by several experiments and measurements. Difference between measured and predicted deviation of observed point position by using our model is smaller than one pixel and is decreasing by increasing distance of observed object from camera.

## REFERENCES

- [1] Alessandri Cozzani, Metteo Appolloni, Stephane Roure, Stephane Beauvivre, Gianluca Casarosa, and Andre Tavares. Measurement and calibration of a prototype miniaturised videogrammetry system in thermal-vacuum. In Fletcher, editor, *Proceedings of the 5th International Symposium on Environmental Testing for Space Programmes Noordwijk*, pages 331–340, August 2004.
- [2] David A. Forsyth and Jean Ponce. *Computer Vision - A Modern Approach*. Prentice Hall, August 2002. 693 pp.
- [3] Richard I. Hartley. In defense of the eight-point algorithm. *IEEE Transactions on pattern analysis and machine intelligence*, 19(6):580–593, June 1997.
- [4] Timo Kahlmann, Fabio Remondino, and H. Ingensand. Calibration for increased accuracy of the range imaging camera swissranger™. In *SPRS Commission V Symposium 'Image Engineering and Vision Metrology'*, volume XXXVI, pages 136–141, Dresden, 25-27 September 2006.
- [5] Peter Podbreznik and Danijel Rebolj. Automatic comparison of site images and the 4D model of the building. In Scherer Raimar J., Katranuschkov Peter, and Schapke Sven-Eric, editors, *CIB W78 22nd conference on information technology in construction*, pages 235–239, Dresden, Germany, July 2005. Institute for Construction Informatics and Technische Universitat and Dresden.
- [6] Peter Podbreznik and Danijel Rebolj. Building elements recognition using site images and 4D model. In Hugues Rivard; Edmond Miresco and Hani Melhem, editors, *Joint international conference on computing and decision making in civil and building engineering*, page 87, Montreal, Canada, June 2006.
- [7] Thierry Sentenac, Yannick Le Maoult, Guy Rolland, and Michel Devy. Temperature correction of radiometric and geometric models for an uncooled CCD camera in the near infrared. *IEEE Transactions on instrumentation and measurement*, 52(1):46–60, February 2003.
- [8] Wikipedia. Coefficient of thermal expansion. [http://en.wikipedia.org/wiki/Coefficient\\_of\\_thermal\\_expansion](http://en.wikipedia.org/wiki/Coefficient_of_thermal_expansion), April 2008.
- [9] Zhengyou Zhang. Determining the epipolar geometry and its uncertainty: A review. *International Journal of Computer Vision*, 2(27):161–198, 1998.

**Peter Podbreznik** Peter Podbreznik, born in 1979, received the diploma degree in 2004 from the University of Maribor. He currently holds a position of PhD student at Faculty of Electrical Engineering and Computer Science and assistant at the Faculty of Civil Engineering, Maribor. His research interests are construction information technologies, segmentation algorithms at computer image processing, pattern recognition and computer vision.

**Božidar Potočnik** Božidar Potočnik, born in 1972, received the Doctor of Science degree in 2000 from the University of Maribor. He currently holds a position of Associate Professor in the Faculty of Electrical Engineering and Computer Science, Maribor. His research interests are segmentation algorithms at computer image processing, pattern recognition, biomedicine, cognitive vision, and machine learning. He is a member of IEEE Computer Society, IEEE Society of Engineering in Medicine and Biology, and Slovenian Pattern Recognition Society.